# Runaway Kaposi Sarcoma-associated herpesvirus replication correlates with systemic IL-10 levels

Carolina Caro-Vegas[a], Subhashini Sellers[b], Kurtis M. Host[a], Jedediah Seltzer[a], Justin Landis[a], William A. Fischer II[b], Blossom Damania[a], Dirk P. Dittmer[a,*]

[a] UNC Lineberger Comprehensive Cancer Center and Department of Microbiology and Immunology, School of Medicine, The University of North Carolina at Chapel Hill, 450 West Drive, Chapel Hill, NC, 27599, USA
[b] Division of Pulmonary Diseases and Critical Care Medicine, School of Medicine, The University of North Carolina at Chapel Hill, 130 Mason Farm Road, Chapel Hill, NC, 27599, USA

ARTICLE INFO

*Keywords:*
KSHV
Kaposi's sarcoma
KICS
Castleman's disease
Herpesvirus
Tocilizumab
IRIS

ABSTRACT

KSHV-associated inflammatory cytokine syndrome (KICS) is caused by Kaposi's sarcoma-associated herpesvirus (KSHV). KICS is associated with high-level, systemic replication of KSHV. This study characterized the clinical and virologic features of a KICS patient over time. Additionally, it compared the cytokine profiles of the KICS case to Kaposi's sarcoma (KS) (n = 11) and non-KS (n = 6) cases. This KICS case presented with elevated levels of KSHV and IL-10, as expected. Surprisingly, this case did not have elevated levels of IL-6 or human immunodeficiency virus 1 (HIV-1). Nevertheless, treatment with anti-IL6 receptor antibody (tocilizumab) reduced KSHV viral load and IL-10. The KSHV genome sequence showed no significant changes over time, except in ORF24. Phylogenetic analysis established this isolate as belonging to KSHV clade A and closely related to other US isolates. These findings suggest IL-10 as potential biomarker and therapy target for KICS.

## 1. Introduction

Kaposi's Sarcoma associated herpesvirus (KSHV), also known as human herpesvirus-8 (HHV8), is the etiologic agent of Kaposi's sarcoma (KS), primary effusion lymphoma (PEL), and the plasmablastic variant of multicentric Castleman disease (KSHV-MCD) (reviewed in (Dittmer and Damania, 2016)). Primary KSHV infections are largely asymptomatic. KSHV-associated malignancies and KSHV reactivation are associated with immune suppression of multiple etiologies, including those that are caused by human immunodeficiency virus (HIV). KS is the single most common cancer in people living with HIV today. KS has a unique clinical manifestation of violaceous lesions in the skin, the respiratory system, and gastrointestinal tract. Interestingly, pediatric KS in a KSHV-endemic region often presents as lymphadenopathy without any skin lesions (El-Mallawany et al., 2019). PEL and KSHV-MCD are B-cell lymphoproliferative disorders caused by KSHV. In KS and PEL, KSHV establishes a latent infection. In KSHV-MCD, KSHV undergoes viral lytic reactivation in a large proportion of KSHV-infected cells. In these three diseases, systemic KSHV viral loads seldom exceed $10^4$ copies/ml (Tamburro et al., 2012). By contrast, KSHV-associated inflammatory cytokine syndrome (KICS) is a clinically-defined disease of KSHV that is associated with very high levels of KSHV in the blood (Polizzotto et al., 2016; Uldrick et al., 2010). KSHV-MCD, KICS and KSHV immune reconstitution syndrome (KS-IRIS) or KS flares share overlapping clinical features, such as lymphadenopathy, cytopenia, and inflammatory symptoms. The symptoms are thought to be secondary to systemically elevated levels of human interleukin 6 and/or viral interleukin 6 secondary to KSHV replication (reviewed in (Oksenhendler et al., 2019; Yu et al., 2017)). Of note, KICS can develop despite control of HIV viremia (Cantos et al., 2017). Thus, KICS is not simply a manifestation of acquired immune deficiency syndrome (AIDS), rather HIV replication and KSHV replication are at times uncoupled.

As KICS and KSHV-MCD share a similar clinical representation, KSHV-MCD must be ruled out by pathologic evaluation before KICS can be diagnosed. Currently, KICS has no established treatment. Treatment strategies similar to KSHV-MCD have been suggested, such as rituximab and liposomal doxorubicin, or high-dose zidovudine and valganciclovir (Lurain et al., 2018; Prieto-Barrios et al., 2018; Uldrick et al., 2011, 2014). Anti-IL6R antibodies such as tocilizumab or anti-IL6 antibodies such as siltuximab have been sporadically explored in MCD, as this treatment has become the standard of care for non-virally associated, idiopathic Castleman's disease (van Rhee et al., 2018). Anti-IL6R therapy has not been tested in KICS.

This report describes a KICS patient treated with anti-IL6R

* Corresponding author.
*E-mail address:* dirk_dittmer@med.unc.edu (D.P. Dittmer).

https://doi.org/10.1016/j.virol.2019.10.002
Received 3 June 2019; Received in revised form 11 September 2019; Accepted 1 October 2019
Available online 02 October 2019

neutralizing antibodies at the University of North Carolina at Chapel Hill. Clinical and laboratory conditions of the KICS patient are compared with a group of eleven KS and HIV-infected patients and six non-KS and HIV-infected patients. The comparison further elucidates the pathogenesis of KICS and suggests IL-10 as a new biomarker for disease progression. Using genome-wide overlapping PCR (AmpliSeq), we obtained the complete KSHV genome sequence from different time points of the disease. These represent one of the few KSHV sequences from circulating genomes, rather than tumor-associated, and potentially defective, KSHV genomes.

## 2. Methods

**Plasma isolation.** 20 mL of whole blood was collected in purple cap EDTA tubes. Samples were centrifuged two times at 400 g for 10 min. Plasma was stored in 1 mL aliquots in matrix tubes (Matrix Technologies Corp. #4252) at -80 °C.

**DNA extraction.** DNA was extracted using a Roche MagNA Pure Compact Instrument (Roche, #03731146001) and Nucleic Acid Isolation Kit I -Large Volume (Roche, #03730972001). 10 µL of a control plasmid, Fly 2.0 (Addgene #117418), was added to each sample to serve as control for DNA extraction efficiency.

**Viral load assay**. Following DNA extraction qPCR was performed on the samples using a 3-primer master mix assay. Primers were designed for KSHV, EBV, and FLY 2.0 and obtained from Europhins Genomics. KSHV: LANA78-F GGAAGAGCCCATAATCTTGC and LANA78(2)-R GCCTCATACGAACTCCAGGT. EBV (Hilscher et al., 2005): EBNA3C-F AAGGTGCATTTACCCCACTG and EBNA3C-R AGCA GTAGCTTGGGAACACC. Fly: Flyflap-f AATCATAAAGCGTTTTAAGCTC CAACGA and Fly Flyflap-r AATCATAATTCCTGACTCCCAAGTGGAC. Individual master mixes were made by adding 20 µL of 5 µM of primer pair to 400 µL of SYBR® Select Master Mix (ThermoFisher/ABI #4472920). 9 µL of DNA sample and 9.9 µl of master mix were used for each well (125 nM final concentration). For each primer pair, we generated an oligonucleotide to serve as a template for creating a copy number standard curve. The oligonucleotide standards (Eurofin Genomics) were diluted to construct standard curves with a starting concentration of 100,000 copies/µL. Reactions were set up using a Freedom Evo 150 robot (Tecan Group Ltd.) in LightCycler® 480 Multiwell 384 Plates (Roche Catalog # 04729749001). PCR reactions were carried out and read with a LightCycler® 480 II/384 (Roche) instrument. Cycle conditions were 95 °C: 5 min, (95 °C: 15 s, 62 °C: 1 min, x40).

**ELISA.** IL-6, IL-8 and IL-10 were quantify using ready-set-go kit (eBioscience) per manufacturer instructions. Plates were washed with plate washer ELx405 (Biotek). Absorbance was measured at 450 nm using spectrophotometer Infinite M200 PRO (Tecan). For DNAse treatment 100 µL of 10x RQ1 buffer (Promega Inc). and 400 µl of water was added to 500 µL of serum. Each sample was treated using 2.5 µL DNAse 1 U/µl and incubated at 37 °C for 30 min. Afterwards, 6 µL of EGTA Stop Buffer was added to the samples and incubated at 65 °C for 10 min prior to automated DNA extraction as describe above.

**Luminex assay and analysis.** Plasma was tested with a human cytokine magnetic 35-plex panel (Life Technologies) per the manufacturer's instructions and analyzed with a MAGPIX instrument (Luminex). R version 3.5.1 was used to conduct analysis and generate figures. Data was scaled and subjected to principle component analysis (PCA) The code is available at: https://bitbucket.org/dittmerlab/r_methods_cytokine/src/master/and the original data are in Supplemental Table 1.

**Viral sequencing and mutation calling.** Total nucleic acid was extracted from 1 mL of plasma as described above and quantitated by Qubit 3.0 dsDNA HS Assay (Life Technologies). Custom Ion Ampliseq primer pools (Life Technologies) were designed to amplify the viral genome using KSHV BAC16 (JSC-1 isolate, GQ994935) as the target. Libraries were prepared from 100 ng total DNA with Ion AmpliSeq Exome RDY Library Preparation Kit (Life Technologies) using protocol MAN00009808 Rev: A.0. Libraries were quantitated by Qubit dsDNA HS Assay, sized with Agilent Bioanalyzer 2100 High Sensitivity DNA Assay (Agilent Technologies), and pooled to 80 pM final concentration. Templating and loading onto the Ion 540 Chip (Life Technologies) were automated on the Ion Chef (Life Technologies). Samples were sequenced on the Ion S5 System (Life Technologies). Base calling was performed on the Ion S5 (Life Technologies) with default parameters.

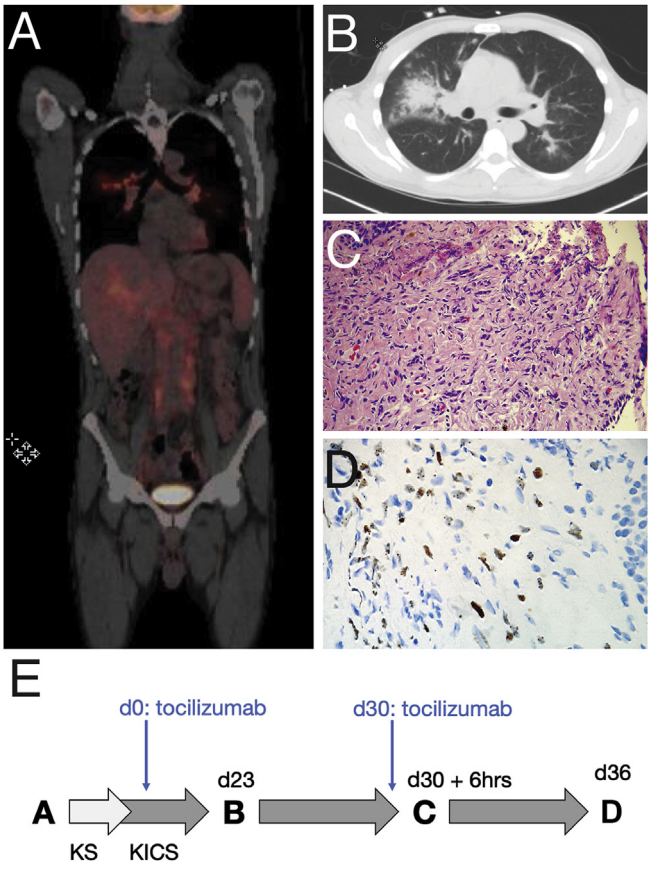


**Fig. 1.** Clinical manifestation of KICS
(A) PET-CT scans demonstrated hypermetabolic lymph nodes in chest, and the (B) CT images taken in the same visit demonstrated presence of pulmonary KS. Histopathology of transbrochial
biopsies showed (C) cancerous arrangement by H&E staining and (D) positive histochemistry for LANA. (E) Timelines of each sample collection and tocilizumab treatment.

Subsequent steps included quality filtering and trimming using bbduk version 37.25 (https://jgi.doe.gov/data-and-tools/bbtools/) (k = 23 mink = 11 ktrim = r hdist = 1 minlength = 50 qtrim = rl trimq = 20 ftl = 10 ftr = 600 maq = 20 tpe tbo). Trimmed reads were mapped to the KSHV genome (NC_009333) using CLC Version 11.0.1 (Qiagen Inc.). Variants were detected using the CLC basic variant detection tool. Only variants that were non-synonymous, minimum average quality score > 19, minimum frequency > 90%, minimum coverage > 40 and forward and reverse balance > 0.05 are reported. For whole viral genome assembly, reads were error corrected and normalized using BBmap (https://jgi.doe.gov/data-and-tools/bbtools/). Next, sequences were aligned to NC_009333 and modified with annotation SOURCE = "NotCoveredByUNCAmpliSeq" to indicate regions of the genome that were not included in the UNC-designed KSHV AmplISeq PCR array using Geneious Prime® 2019.1 (Biomatters Ltd ). Multiple best matches were mapped randomly, and a consensus was built based on majority calls at a minimum read coverage of N = 5. Thereafter the consensus was inspected and poly-nucleotide runs corrected to restore full-length orfs. In an additional step, the error-corrected reads were remapped against these consensus sequences and the

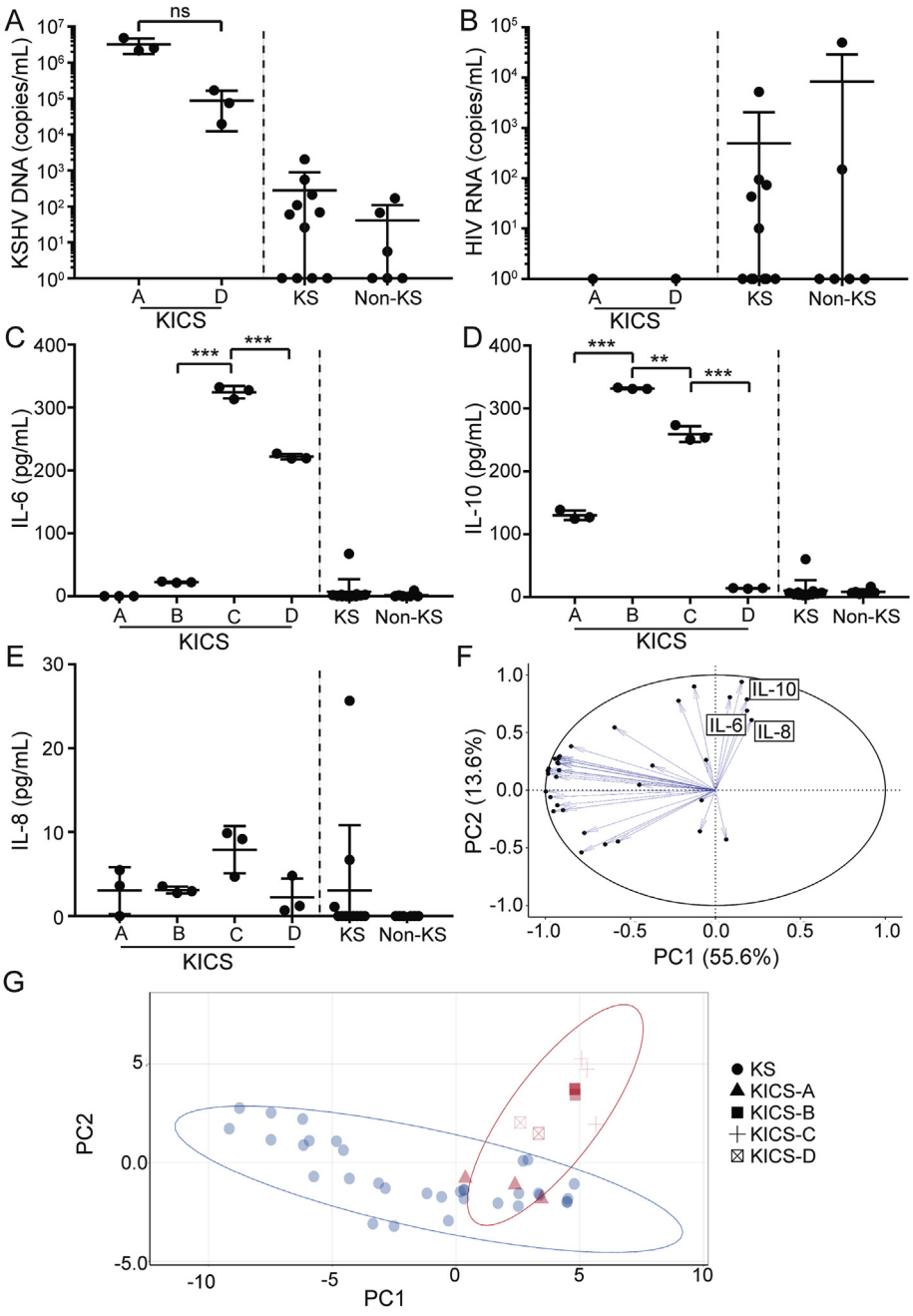


**Fig. 2.** Systemic viral and cytokine levels in the KICS patient in comparison to KS and non-KS cases A = Before KICS was established, patient was only diagnosed with KS, B = After KICS diagnosis, C = day 30, D = day 36. (A) KSHV DNA and (B) HIV RNA levels in plasma from KICS patient at different timepoints A, B, C and D and KS (n = 11) and non-KS patients (n = 6). (C) IL-6, (D) IL-10 and (E) IL-8 on patient plasma, measure by ELISA. For KICS, data represents the mean ± SD of n = 3 independent experiments of each plasma sample. For KS and non-KS, each data point represents the mean of n = 3 independent measurements, the mean ± SD was calculated of the entire group (KS n = 11 and non-KS n = 6). Principal component analysis of the 34-cytokine measured by Luminex that characterizes (F) the mayor drivers and (G) compares KICS and KS.

final consensuses were obtained. Gaps were repaired from the target to restore open reading frames (annotated). In-frame Indels and SNV were maintained. Six regions of the KSHV genome were not covered by AmpliSeq primers: 24,213–25,057 (845 bp), 113949–114,092 (144 bp), 117,733–118,873 (1141 bp), 120,140–120,301 (162bp), 124,968–126,099 (1,132bp), and 137,588–137,917 (330 bp). Here, the sequence from GQ994935 was inserted. The sequences are available in GenBank (MK733606: UNC_KICS009, MK733608: UNC_KICS010, MK733609: UNC_BAC16, MK733607: UNC_BC1). Coverage analysis was conducted in R v3.6.0. Raw counts at each position were normalized by applying a cube-root transformation, followed by log10 transformation after (+1) was added to positions were counts where 0. Next, the data were median-centered and a rolling window was applied to calculate the median across 99 bp with an overlap of 33 bp. The code and data are available at https://bitbucket.org/dittmerlab/kics2018/src/master/.

**Phylogenetic analysis.** To compare our KSHV isolate to existing whole genome data, the following sequences were used: NC009333, LC200589, LC200588, LC200587, LC200586, AP017458, U93872, KT271468, KT271467, KT271466, KT271465, KT271464, KT271463, KT271462, KT271461, KT271460, KT271459, KT271458, KT271457, KT271456, KT271455, KT271454, KT271453, GQ994935, KF588566, JQ619843, JX228174, HQ404500 and AF148805. KICS patient sequences are indicated as consensus09 and consensus10. Full-length consensus by majority vote genomic sequences, obtained after single pass mapping of trimmed, error-corrected reads were used to generate a multiple alignment using MAFFT (Katoh and Standley, 2013) with default options. The tree was generated using Geneious Prime® 2019.1 (https://www.geneious.com/) based on Jukes-Canter Distance and a neighbor-joining algorithm with no outgroup. A consensus was generated by bootstrapping (n = 100). K1 sequence protein alignment was based on 440 sequences in GenBank and also generated MAFFT with BLOSUM62 matrix and visualized the same way.

**Statistics.** Results are reported as mean ± SD. All cellular

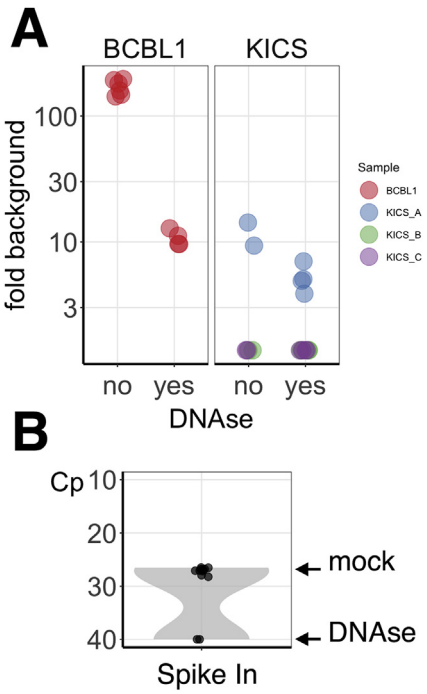


**Fig. 3.** A substantial fraction of circulating DNA is virion encapsulated
(A) Shown are relative levels of KSHV DNA, on a log 10 scale, as detected by real-time QPCR on the vertical axis for samples with or without DNAse treatment (horizontal axis). The colors indicate the different samples. For each sample multiple replicates are shown. DNAse treatment was significant to $p \leq 0.001$ by two-way ANOVA ($n = 25$). The patient samples were: A = Before KICS was established, patient was only diagnosed with KS (blue), B = After KICS diagnosis (green), C = day 30 (purple), D = not available. BCBL1 = induced supernatant from BCBL1TREX (red). (B) Violin plot. Shown on the vertical axis are raw Cp values for spiked in, naked control DNA either DNAse or mock treated.

experiments were repeated in at least three complete biological replicates. Unpaired 2-tailed t-test with Welch correction (not assuming equal variance) was used to compare groups.

**Study approval.** Studies were approval by internal review board (IRB) of the University of North Carolina, Chapel Hill, North Carolina, USA.

## 3. Results

### 3.1. Clinical presentation

The patient was a 45-year old male with HIV, who had initiated treatment with an integrase inhibitor-based antiretroviral regimen when he presented with dyspnea, fevers and violaceous skin lesions. Skin biopsy confirmed KS. He was admitted one month later with disease progression. At that time, a computed tomography scan of the chest demonstrated lung lesions thought to be pulmonary KS. The patient had recurrent episodes of fever and pancytopenia. As repeated infectious evaluations were negative, these signs were thought to be secondary to KS-IRIS. After initiating treatment with doxorubicin, he had clinical improvement. Eight months later, his KS progressed and required a change in treatment to paclitaxel. The patient was readmitted with shortness of breath, fatigue, pancytopenia and fevers. He underwent a bronchoscopy with transbronchial biopsies confirming pulmonary KS (Fig. 1A and B). KS biopsy was positive for LANA stain (Fig. 1C and D). He was believed to have KICS rather than KS-IRIS and treated with tocilizumab, a humanized monoclonal antibody against the interleukin-6 receptor (IL-6R) that is approved for classic CD, with good initial response. However, his health continued to decline despite the addition of humanized monoclonal antibody against CD20 $^{+}$ B cells (rituximab) to his treatment regimen.

Blood samples from four different time points were available for analysis (Fig. 1E): (A) Day 0, patient was diagnosed with KS, (B) day 23, patient was diagnosed with KICS and had received first dose of tocilizumab 23 days earlier, (C) day 30, 1 h after patient received a second dose of tocilizumab and (D) day 36, i.e. six days after patient was treated with two doses of tocilizumab. The laboratory data of the KICS patient were compared to twelve KS/HIV-positive and six non-KS/HIV-positive lymphoma patients. All patients were male ranging from 28 to 59 years. The non-KS group included two cases with B-cell lymphoma, two diffuse large B-cell lymphoma, and two Hodgkin's lymphomas.

### 3.2. KICS patient had high levels of KSHV, but not HIV

At diagnosis (time point A), the patient had a KSHV viral load (total DNA) of $2.4 \times 10^6$ copies/mL, which decreased to $6.7 \times 10^5$ copies/mL at the end of study (time point D). The intermediate time points failed PCR extraction control and could not be analyzed. The KS group and non-KS group had an average of 280 copies/mL and 40 copies/mL of KSHV plasma DNA respectively, i.e. about a 3 $_{10}$log lower than the lowest KICS value (Fig. 2A). Approximately half of the DNA signal was protected from DNAse I digestion (Fig. 3A) at time point A. No clinical material was left to conduct the same experiment for the other time points. In comparison greater than 80% of the DNA signal obtained from induced BCBL T-REx cells was DNAse sensitive. Exogenously added DNA served as control for DNAse activity and absence of DNAse inhibitors in serum (Fig. 3B). The KICS patient had an undetectable HIV viral load at all timepoints, while HIV viral load across the KS group ranged from undetectable to $5.2 \times 10^3$ copies/mL and across the non-KS group from undetectable to $5.0 \times 10^4$ copies per mL (Fig. 2B). Thus, this case uncouples high-level KSHV replication from high-level HIV replication.

### 3.3. KICS could be differentiated from KS by its cytokine profile

To test the hypothesis that cytokine levels correlate with KICS and can be used to follow treatment, we measured (i) human IL-6, IL-10 and IL-8 by ELISA and (ii) a panel of 34 cytokines by Luminex in the KICS patient at timepoints A, B, C, and D, as well as in the KS positive ($n = 11$), and KS-negative ($n = 6$) cancer patients with HIV. Historically, high levels of IL-6 are associated with KICS; however, this patient did not exhibit elevated levels of IL-6 at time of KICS diagnosis (time point A (KS) undetectable, time point B (KICS diagnosios). 22 pg/mL). IL-6 reactivity in ELISA increased 10-fold upon treatment with tocilizumab: to 324 pg/mL at 23 days after dose 1 (time point C), and 222 pg/mL at 6 days after dose 2 (time point D) (Fig. 2C). IL-10 increased 3-fold after the patient was clinically diagnosed with KICS to 331 pg/mL (time point B), compared to KS (130 pg/mL (time point A), remained level after a single dose of tocilizumab (time point C) followed by a drastic decrease at day 6 after the second tocilizumab treatment (time point D) (Fig. 2D). The KICS patient did not show substantial IL-8 levels at any of the timepoints (Fig. 2E). None of the patients in the KS or non-KS groups presented with elevated values of any of the three cytokines, confirming IL-6 and IL-10 as closely associated with KICS.

Luminex-based multiplex analysis was used to study a broader range of cytokines. Principal component analysis identified IL-6 and IL-10 as the main cytokines driving the difference between KS and KICS on the one hand and between the different stages of KICS (PC1). TNF and IL-9, and pro-inflammatory cytokines were the main drivers of PC2 (Fig. 2F), which represents the difference between KS and non-KS. Together, PC1 and PC2 explained 69.2% of the variation in the data. It was possible to differentiate KICS from KS on the basis of cytokine profiling and monitor disease progression (Fig. 2G, different shapes indicate the different time points). This confirms IL-6 as a diagnostic marker for

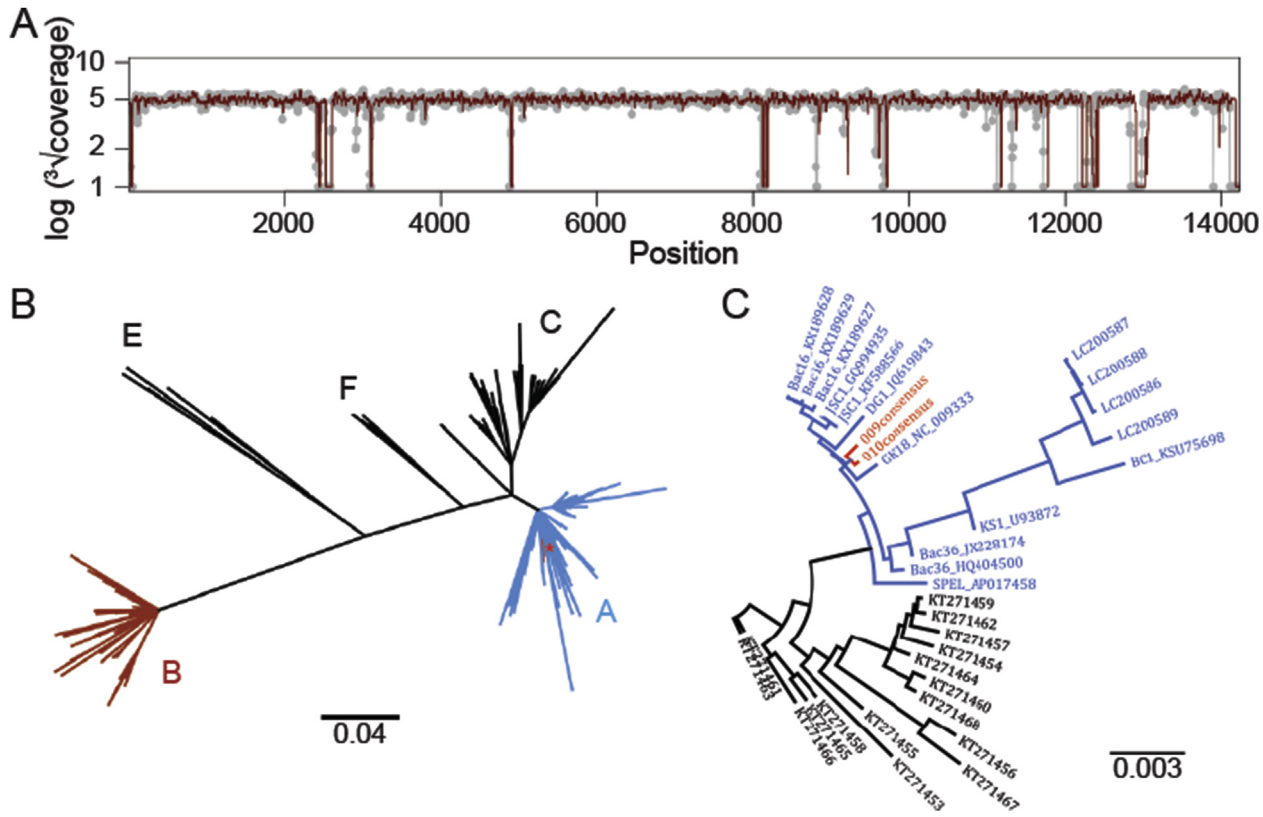


**Fig. 4.** NextGen-sequencing analysis of KICS patient at different timepoints
(A) Distribution of reads that align to KSHV (NC009333) genome. Timepoint A in red (before KICS was established) and timepoint B in grey (after KICS was diagnosed). Phylogenetic trees demonstrating alignment of generated consensus sequences for KSHV isolated from patient plasma, in comparison to (B) established KSHV K1 clades and (C) previously reported KSHV sequences (A = 09 consensus and B = 10 consensus, highlighted in red).

KICS and suggests that measuring IL-10 in addition may improve disease monitoring and differential diagnosis.

### 3.4. KSHV genomes in KICS

We used PCR-based enrichment (AmpliSeq) and Ion Torrent chemistry to determine the complete genome sequence of KSHV circulating in this patient (submitted to GenBank). High-confidence whole genomes were obtained for timepoints A and B, where KSHV viral loads were high ($\geq 10^5$ copies/ml). 1,381,470 raw reads aligned to KSHV for time point A yielding a mean coverage of 96.5 ± 36.9-fold (Q20 = 94.1%) covering 94.8% of the reference sequence with 91% identical sites. 3,769,841 raw reads aligned to KSHV for time point B yielding a mean coverage of 99.1 ± 35.4-fold (Q20 = 94%) covering 95.7% of the reference sequence with 90.8% identical sites. Time point C did not have enough reads to cover the entire genome despite repeated attempts. Only 59.2% of the reference sequence was covered to 38.8 ± 46.9-fold coverage (Q20 = 95.2%). Of that 91.7% were identical to the reference sequence. We also sequenced the KSHV out of PBMC from these same time points. Time point D was virus negative. This mapping used the KSHV reference sequence NC_009333 (Fig. 4A). As positive control KSHV BAC16 and KSHV from BC1 cells were re-sequenced. Six regions (see methods) were not covered by this AmpliSeq array. Every region contained in the array yielded mappable reads, suggesting that no large-scale deletions or rearrangements had occurred.

Independent of the whole genome assembly all reads were used for single nucleotide variant (SNV) calling using high-confidence parameters as established for human SNV typing (Table 1). No InDels or SNV were identified that were present in sample A and absent in sample B. A number of SNV, relative to the consensus sequence were consistently observed at both time points. At time point C, sequence coverage was fragmented. Hence, a number of A/B-specific SNV could not be confirmed. Notably, a series of three SNV in ORF24 were observed only at time point C, but not at time points A and B. The majority of non-synonymous SNV were shared with viral sequences obtained from sequencing PBMC. Whether any of the sequence differences have functional consequences remains to be explored. Based on a comparison of 29 full length KSHV genome sequences, this isolate aligned to the Western-European AIDS- PEL- and KS-derived sequences. More specifically, both sequences aligned with clade A, shown in blue (Fig. 4B). It suggests that the current KSHV reference sequence represents a complete viral genome. In sum, this KICS case represented a rare and much needed scientific opportunity to obtain complete KSHV genome information, pertaining to viral strains of demonstrated *in vivo* replication potential and human infectivity.

## 4. Discussion

KICS represents the most aggressive and fatal outcome of KSHV infection. KICS is convincingly associated with systemic high-level KSHV replication and a cytokine storm dominated by IL-6 and IL-10 (Polizzotto et al., 2016; Uldrick et al., 2010). It is likely that these cytokines are the mechanistic drivers of the clinical disease phenotype, and they may constitute a target to ameliorate symptoms. Due to the similarities between KICS and KSHV-MCD, treatments with efficacy in KSHV-MCD may also have efficacy in KICS, although the accelerated clinical course of KICS typically requires more aggressive interventions. Further studies are needed to understand the biology of KICS and to differentiate KICS from KSHV-MCD or KS-IRIS.

This particular KICS patient did not present elevated levels of IL-6. Instead, IL-10 stood out as the clinical measurement that in addition to

**Table 1**
Summary of non-synonymous mutations.

| Pos(1) | Ref | Mut | Pos(1) | Ref | Mut | Time Bloos Point(3) | Time PBMC Point(4) | Name | Function(2) |
|---|---|---|---|---|---|---|---|---|---|
| 168 | CA | TT | 22 | gln | leu | A, B, C | A, B, C | K1 | Signaling |
| 181 | A | C | 26 | asn | thr | A, B, C | A, B, C | | |
| 183 | C | T | 27 | leu | phe | A, B, C | A, B, C | | |
| 570 | G | A | 155 | ala | thr | .,., . | A, B, C | | |
| 609 | C | A | 169 | leu | ile | A, B, ND | A, B, C | | |
| 619 | C | G | 172 | ser | trp | A, B, ND | A, B, C | | |
| 699-761 | | | 199-219 | | | | | | (5) |
| 2414 | G | T | 435 | ala | ser | A, B, C | A, B,. | ORF4 | complement binding |
| 3263 | G | C | 29 | val | leu | A, B, ND | A, B, C | ORF6 | ssDNA binding |
| 4364 | G | A | 396 | val | met | A, B, C | A, B, C | | |
| 5663 | G | C | 829 | asp | his | .,., . | A, B, C | | |
| 5844 | T | C | 889 | val | ala | ., B, ND | A, B,. | | |
| 6831 | A | G | 80 | thr | ala | A, B, C | A, B,. | ORF7 | unknown |
| 6901 | T | C | 103 | ile | thr | A, B, ND | A, B, C | | |
| 8517 | A | G | 642 | lys | glu | A, B, C | A, B, C | | |
| 14322 | C | G | 998 | ile | met | A,., ND | A, B, C | ORF9 | DNA polymerase |
| 15084 | G | T | 200 | met | ile | A, B, ND | A, B,. | ORF10 | unknown |
| 15093 | A | C | 203 | glu | asp | A, B, ND | A, B, C | | |
| 15116 | C | A | 211 | pro | gln | A, B, ND | .,., . | | |
| 15164 | A | G | 227 | tyr | cys | A, B, ND | A, B, C | | |
| 15078 | C | T | 232 | his | tyr | .,., . | A, B, C | | |
| 15214 | A | G | 244 | ile | val | A, B, ND | A, B, C | | |
| 15408 | C | T | 308 | glu | asp | .,., . | A, B, C | | |
| 15497 | C | T | 338 | thr | ile | .,., . | A, B,. | | |
| 15662 | A | G | 393 | his | arg | A, B, C | A, B,. | | |
| 15906 | A | C | 51 | asn | his | A, B, C | A, B, C | ORF11 | unknown |
| 17268 | T | C | 192 | asn | asp | A, B, C | .,., . | K2 | DHFR |
| 17817 | T | G | 9 | ile | leu | A, B, C | A, B, C | | |
| 17838 | G | A | 2 | arg | cys | A, B, C | A, B, C | | |
| 18647 | A | G | 299 | leu | pro | A, B, ND | A, B,. | K3 | |
| 32659 | A | G | 46 | lys | arg | A, B, C | A, B, C | | unknown |
| 33960 | G | A | 328 | ala | val | A, B, C | A, B, C | ORF19 | unknown |
| 35959 | G | T | 160 | gly | cys | A, B, ND | A, B, C | ORF21 | TK |
| 41515 | T | A | 455 | asn | leu | .,., C | .,., . | ORF24 | unknown |
| 41518 | T | A | 454 | asn | leu | .,., C | .,., . | | |
| 41521 | – | A | 453 | fs | fs | .,., C | .,., . | | |
| 61287 | C | T | 294 | thr | ile | A, B, C | .,., C | ORF40 | helicase-primase |
| 99622 | G | A | 227 | pro | ser | A, B, C | .,., . | ORF61 | assembly |
| 131763 | T | C | 943 | ile | val | A,., ND | .,., . | orf75 | FGARAT Homolog |
| 135059 | A | G | 412 | leu | pro | A, B, ND | A, B,. | K15 | Signaling |
| 135882 | T | G | 221 | ser | arg | ., B, ND | A, B, C | | |

(1) Based on sequence GenBank ID: NC_009333.
(2) Based on original assignment by Russo et al. (1996) these refer to enzymatic functions that are conserved across herpesviruses and implicated in virus replication. Function is inferred from sequence similarity across multiple homologous herpesviruses, not necessarily experiments. Conversely, many of the genes labeled "unknown" function have shown specific activities in selective bioassays.
(3) Time point at which SNV was detected with high confidence in DNA isolated from plasma: A, B, C. The symbol "." indicates the absence of the SNV at that time point; "ND" indicates that no reliable sequence information was available at that time-point.
(4) Time point at which SNV was detected with high confidence in DNA isolated from PBMC: A′, B′, C.' The symbol "." indicates the absence of the SNV at that time point; "ND" indicates that no reliable sequence information was available at that time-point.
(5) The complex repeat region in K1 was not resolved in virus isolated from plasma.

KSHV DNA copy number lead to the diagnosis of KICS. KSHV DNA copy number decreased after treatment. Treatment also reduced IL-10 levels, whereas IL-6 increased after tocilizumab was administered. Thus IL-10, rather than IL-6 served as a better biomarker to follow disease progression after tocilizumab treatment of KICS. Because tocilizumab is an IL-6 receptor inhibitor (reviewed in (Nishimoto and Kishimoto, 2004)), it may have interfered with the IL-6 ELISA. Alternatively, IL-6, even though present at high levels, may have had no biological activity on IL6 receptor signaling due to the presence of tocilizumab. The relationship between huIL6 and sIL6-R is quite complex. For instance, native sIL6R serves to extend the half-life of IL6 in solution and enhances binding. Furthermore, soluble gp130 also exists at measurable concentrations in blood. It is not entirely clear how adding anti-IL-6R antibodies changes this equilibrium with regard to biology or diagnostic assay performance. Whether tocilizumab also affected viral IL6 signaling and what the viral IL6 levels were in this case is unknown due to the low volume of sample and lack of reagents. Further studies to evaluate the use of IL-10 as a biomarker for KICS seem warranted.

We successfully sequenced a KSHV genome from patient plasma, rather than tumor tissue. Thus, this study contributes to the community collection of whole genome KSHV sequences, which is still the most limited among all herpesviruses (Brulois et al., 2012; Olp et al., 2015; Russo et al., 1996; Sallah et al., 2018; Tamburro et al., 2012; Yakushko et al., 2011). The sequencing data support the completeness of the current KSHV reference sequence. Pre-NGS enrichment represented an efficient method to sequence KSHV in the background of contaminating human DNA and allowed full-length sequencing from KSHV from PBMC. It did little, however, to overcome the dependence on high viral genome copy number ($10^5$ copies/sample) in serum. Lower KSHV input copy numbers yielded only partial genomes and are likely to suffer from PCR bias. We were unable to design capture primers to the repeat regions of the KSHV genome. Hence, the number of and sequence of repeats reported reflects the current reference genome and is likely an underestimation of the true number of repeats (Lagunoff and Ganem,

1997).

It is conceivable that a specific mutation in the KSHV genome is associated with a high replicative phenotype during KICS (Ray et al., 2012). We were not able to identify a significant SNV that differed from consensus A (before KICS was diagnosed) and consensus B (after KICS was officially diagnosed). A limitation was unequal genome coverage, as a higher mean genome coverage was obtained from PBMC due to advances in sequencing technology. As expected, the virus had low genetic variation over time and when compared to the reference genome. The exception being the variable regions in K1. Whether any of the non-synonymous SNV could have impacted viral replication is the subject of future studies. As this study sequenced total DNA rather than encapsulated, virion DNA, it most likely reflects a mixture of virion DNA and fragments of viral DNA, released by dying cells. In support of this assessment, some SNV were seen in sequences obtain from serum DNA at multiple time points, but not in the corresponding DNA obtained from PBMC and vice versa, e.g. K1 at aa 155 or orf10 at aa 211.

Alternatively, the patient's genome could harbor SNV that predisposed him to KSHV infection or resulted in a suboptimal response to viral reactivation. Here, the interpretive value of a single case study is necessarily limited. Whole Exome sequencing yielded 1979 previously reported homozygous SNV, of which 338 were annotated in ClinVar. We do not know the significance of any of them, but these included biologically plausible candidates SNV in genes such as IL-4R, IL-13, TRL1 or TAB2.

The patient presented in this study was HIV seropositive, but at the time had no detectable HIV viral load. This was unexpected if one considers KSHV-associated malignancies in the context of late-state AIDS, as during the 1990 epidemic in US and European men who have sex with men Centers for Disease (1981); however, KS has since become appreciated as a much more varied disease entity. Particularly in KSHV-endemic regions, KS is independent of HIV viral load and CD4 counts (Hosseinipour et al., 2014). In the same setting, IL6 and IL10 are often elevated in pediatric KS with lymph node involvement and KSHV-MCD is seen more frequently than previously assumed, reinforcing the connection between KSHV replication and KSHV-induced pathology in the lymphoid compartment. In summary, clinical complications and malignancies associated with KSHV infection have become more varied. A better understanding of viral pathogenesis is needed to validate clinically relevant biomarkers and discover novel interventions.

## Declaration of competing interest

The authors have declared that no conflict of interest exists.

## Acknowledgments

This work was supported by public health service grants CA163217 and CA239583 to DPD and CA0190014 and CA228172 to BD. The authors thank Razia Moorad for critical reading and contributing to the sequence analysis, Tischan Seltzer for critical reading, and the Dittmer and Damania labs for cheerful discussions. The authors thank the patient and his family for participation in this study.

## Appendix A. Supplementary data

Supplementary data to this article can be found online at https://doi.org/10.1016/j.virol.2019.10.002.

## Author contributions

CC designed and performed experiments, analyzed data, and wrote the manuscript. SS wrote clinical section of manuscript and obtained clinical images of the patient. KH performed the Luminex assay and JL performed the Luminex analysis. JS performed the viral loads assay. WF obtained the clinical sample for this study. BD and DPD designed experiments, analyzed data and contributed to the final version of the manuscript. All authors approved the final manuscript.

## Summary of mutations

(1) Based on sequence GenBank ID: NC_009333
(2) Based on original assignment by Russo et al. (1996)
(3) Time point at which SNV was detected with high confidence: A, B, C. The symbol "." indicates the absence of the SNV at that time point; "ND" indicates that no reliable sequence information was available at that time-point.

## References

Brulois, K.F., Chang, H., Lee, A.S., Ensser, A., Wong, L.Y., Toth, Z., Lee, S.H., Lee, H.R., Myoung, J., Ganem, D., Oh, T.K., Kim, J.F., Gao, S.J., Jung, J.U., 2012. Construction and manipulation of a new Kaposi's sarcoma-associated herpesvirus bacterial artificial chromosome clone. J. Virol. 86, 9708–9720.

Cantos, V.D., Kalapila, A.G., Ly Nguyen, M., Adamski, M., Gunthel, C.J., 2017. Experience with Kaposi sarcoma herpesvirus inflammatory cytokine syndrome in a large urban HIV clinic in the United States: case series and literature review. Open Forum Infect Dis 4, ofx196.

Centers for Disease, C., 1981. Kaposi's sarcoma and Pneumocystis pneumonia among homosexual men–New York City and California. MMWR Morb. Mortal. Wkly. Rep. 30, 305–308.

Dittmer, D.P., Damania, B., 2016. Kaposi sarcoma-associated herpesvirus: immunobiology, oncogenesis, and therapy. J. Clin. Investig. 126, 3165–3175.

El-Mallawany, N.K., Mehta, P.S., Kamiyango, W., Villiera, J., Peckham-Gregory, E.C., Kampani, C., Krysiak, R., Sanders, M.K., Caro-Vegas, C., Eason, A.B., Ahmed, S., Schutze, G.E., Martin, S.C., Kazembe, P.N., Scheurer, M.E., Dittmer, D.P., 2019. KSHV viral load and Interleukin-6 in HIV-associated pediatric Kaposi sarcoma-Exploring the role of lytic activation in driving the unique clinical features seen in endemic regions. Int. J. Cancer 144, 110–116.

Hilscher, C., Vahrson, W., Dittmer, D.P., 2005. Faster quantitative real-time PCR protocols may lose sensitivity and show increased variability. Nucleic Acids Res. 33, e182.

Hosseinipour, M.C., Sweet, K.M., Xiong, J., Namarika, D., Mwafongo, A., Nyirenda, M., Chiwoko, L., Kamwendo, D., Hoffman, I., Lee, J., Phiri, S., Vahrson, W., Damania, B., Dittmer, D.P., 2014. Viral profiling identifies multiple subtypes of Kaposi's sarcoma. mBio 5, 01614 e01633.

Katoh, K., Standley, D.M., 2013. MAFFT multiple sequence alignment software version 7: improvements in performance and usability. Mol. Biol. Evol. 30, 772–780.

Lagunoff, M., Ganem, D., 1997. The structure and coding organization of the genomic termini of Kaposi's sarcoma-associated herpesvirus. Virology 236, 147–154.

Lurain, K., Yarchoan, R., Uldrick, T.S., 2018. Treatment of Kaposi sarcoma herpesvirus-associated multicentric castleman disease. Hematol. Oncol. Clin. N. Am. 32, 75–88.

Nishimoto, N., Kishimoto, T., 2004. Inhibition of IL-6 for the treatment of inflammatory diseases. Curr. Opin. Pharmacol. 4, 386–391.

Oksenhendler, E., Boutboul, D., Galicier, L., 2019. Kaposi sarcoma-associated herpesvirus/human herpesvirus 8-associated lymphoproliferative disorders. Blood 133, 1186–1190.

Olp, L.N., Jeanniard, A., Marimo, C., West, J.T., Wood, C., 2015. Whole-genome sequencing of kaposi's sarcoma-associated herpesvirus from Zambian kaposi's sarcoma biopsy specimens reveals unique viral diversity. J. Virol. 89, 12299–12308.

Polizzotto, M.N., Uldrick, T.S., Wyvill, K.M., Aleman, K., Marshall, V., Wang, V., Whitby, D., Pittaluga, S., Jaffe, E.S., Millo, C., Tosato, G., Little, R.F., Steinberg, S.M., Sereti, I., Yarchoan, R., 2016. Clinical features and outcomes of patients with symptomatic Kaposi sarcoma herpesvirus (KSHV)-associated inflammation: prospective characterization of KSHV inflammatory cytokine syndrome (KICS). Clin. Infect. Dis. 62, 730–738.

Prieto-Barrios, M., Aragon-Miguel, R., Tarrago-Asensio, D., Lalueza, A., Zarco-Olivo, C., 2018. Human herpesvirus 8-associated inflammatory cytokine syndrome. JAMA Dermatol 154, 228–230.

Ray, A., Marshall, V., Uldrick, T., Leighty, R., Labo, N., Wyvill, K., Aleman, K., Polizzotto, M.N., Little, R.F., Yarchoan, R., Whitby, D., 2012. Sequence analysis of Kaposi sarcoma-associated herpesvirus (KSHV) microRNAs in patients with multicentric Castleman disease and KSHV-associated inflammatory cytokine syndrome. J. Infect. Dis. 205, 1665–1676.

Russo, J.J., Bohenzky, R.A., Chien, M.C., Chen, J., Yan, M., Maddalena, D., Parry, J.P., Peruzzi, D., Edelman, I.S., Chang, Y., Moore, P.S., 1996. Nucleotide sequence of the Kaposi sarcoma-associated herpesvirus (HHV8). Proc. Natl. Acad. Sci. U. S. A. 93, 14862–14867.

Sallah, N., Palser, A.L., Watson, S.J., Labo, N., Asiki, G., Marshall, V., Newton, R., Whitby, D., Kellam, P., Barroso, I., 2018. Genome-wide sequence analysis of Kaposi's Sarcoma-associated Herpesvirus shows diversification driven by recombination. J. Infect. Dis. 218 (11), 1700–1710. https://doi.org/10.1093/infdis/jiy427. PubMed PMID: 30010810; PubMed Central PMCID: PMC6195662.

Tamburro, K.M., Yang, D., Poisson, J., Fedoriw, Y., Roy, D., Lucas, A., Sin, S.H., Malouf, N., Moylan, V., Damania, B., Moll, S., van der Horst, C., Dittmer, D.P., 2012. Vironome of Kaposi sarcoma associated herpesvirus-inflammatory cytokine syndrome in an AIDS patient reveals co-infection of human herpesvirus 8 and human herpesvirus 6A. Virology 433, 220–225.

Uldrick, T.S., Polizzotto, M.N., Aleman, K., O'Mahony, D., Wyvill, K.M., Wang, V., Marshall, V., Pittaluga, S., Steinberg, S.M., Tosato, G., Whitby, D., Little, R.F., Yarchoan, R., 2011. High-dose zidovudine plus valganciclovir for Kaposi sarcoma herpesvirus-associated multicentric Castleman disease: a pilot study of virus-activated cytotoxic therapy. Blood 117, 6977–6986.

Uldrick, T.S., Polizzotto, M.N., Aleman, K., Wyvill, K.M., Marshall, V., Whitby, D., Wang, V., Pittaluga, S., O'Mahony, D., Steinberg, S.M., Little, R.F., Yarchoan, R., 2014. Rituximab plus liposomal doxorubicin in HIV-infected patients with KSHV-associated multicentric Castleman disease. Blood 124, 3544–3552.

Uldrick, T.S., Wang, V., O'Mahony, D., Aleman, K., Wyvill, K.M., Marshall, V., Steinberg, S.M., Pittaluga, S., Maric, I., Whitby, D., Tosato, G., Little, R.F., Yarchoan, R., 2010. An interleukin-6-related systemic inflammatory syndrome in patients co-infected with Kaposi sarcoma-associated herpesvirus and HIV but without Multicentric Castleman disease. Clin. Infect. Dis. 51, 350–358.

van Rhee, F., Voorhees, P., Dispenzieri, A., Fossa, A., Srkalovic, G., Ide, M., Munshi, N., Schey, S., Streetly, M., Pierson, S.K., Partridge, H.L., Mukherjee, S., Shilling, D., Stone, K., Greenway, A., Ruth, J., Lechowicz, M.J., Chandrakasan, S., Jayanthan, R., Jaffe, E.S., Leitch, H., Pemmaraju, N., Chadburn, A., Lim, M.S., Elenitoba-Johnson, K.S., Krymskaya, V., Goodman, A., Hoffmann, C., Zinzani, P.L., Ferrero, S., Terriou, L., Sato, Y., Simpson, D., Wong, R., Rossi, J.F., Nasta, S., Yoshizaki, K., Kurzrock, R., Uldrick, T.S., Casper, C., Oksenhendler, E., Fajgenbaum, D.C., 2018. International, evidence-based consensus treatment guidelines for idiopathic multicentric Castleman disease. Blood 132 (20), 2115–2124. https://doi.org/10.1182/blood-2018-07-862334.

Yakushko, Y., Hackmann, C., Gunther, T., Ruckert, J., Henke, M., Koste, L., Alkharsah, K., Bohne, J., Grundhoff, A., Schulz, T.F., Henke-Gendo, C., 2011. Kaposi's sarcoma-associated herpesvirus bacterial artificial chromosome contains a duplication of a long unique-region fragment within the terminal repeat region. J. Virol. 85, 4612–4617.

Yu, L., Tu, M., Cortes, J., Xu-Monette, Z.Y., Miranda, R.N., Zhang, J., Orlowski, R.Z., Neelapu, S., Boddu, P.C., Akosile, M.A., Uldrick, T.S., Yarchoan, R., Medeiros, L.J., Li, Y., Fajgenbaum, D.C., Young, K.H., 2017. Clinical and pathological characteristics of HIV- and HHV-8-negative Castleman disease. Blood 129, 1658–1668.